Marquette University

e-Publications@Marquette

Mechanical Engineering Faculty Research and Publications

Mechanical Engineering, Department of

7-2014

Detailed Computational Modeling of Laminar and Turbulent Sooting Flames

Adhiraj Dasgupta
The Pennsylvania State University

Somesh Roy
Marquette University, somesh.roy@marquette.edu

Daniel C. Haworth
The Pennsylvania State University

Detailed Computational Modeling of Laminar and Turbulent Sooting Flames

Adhiraj Dasgupta
Department of Mechanical and Nuclear Engineering, The Pennsylvania State University, University Park, PA

Somesh Roy
Department of Mechanical and Nuclear Engineering, The Pennsylvania State University, University Park PA

Daniel C. Haworth
Department of Mechanical and Nuclear Engineering, The Pennsylvania State University, University Park PA

ABSTRACT

This study reports development and validation of two parallel flame solvers with soot models based on the open-source computation fluid dynamics (CFD) toolbox code **OpenF0AM.** First, a laminar flame solver is developed and validated against experimental data. A semi-empirical two-equation soot model and a detailed soot model using a method of moments with interpolative closure (MOMIC) are implemented in the laminar flame solver. An optically thin radiation model including gray soot radiation is also implemented. Preliminary results using these models show good agreement with experimental data for the laminar axisymmetric diffusion flame studied. Second, a turbulent flame solver is developed using Reynolds-averaged equations and transported probability density function (tPDF) method. The MOMIC soot model is implemented on this turbulent solver. A sophisticated photon Monte-Carlo (PMC) model with line-by-line spectral radiation database for modeling is also implemented on the turbulent solver. The validation of the turbulent solver is under progress. Both the solvers show good scalability for a moderate-sized chemical mechanism, and can be expected to scale even more strongly when larger chemical mechanisms are used.

Keywords

1. INTRODUCTION

Soot or combustion-generated particulate carbon is a major pollutant, whose effects are felt on various issues ranging from public health to climate change [6, 35]. In some combustion devices, such as in industrial furnaces, where the main objective is to attain high heat transfer rates, the formation of soot may be somewhat 'beneficial' in promoting heat transfer by radiation. But such devices must ensure that overall emission of soot from the system is minimized. Therefore control of soot emission is important in combustion applications.

Combustion involve complex interactions of flow, chemistry, and heat transfer processes. The effect of flow field influences local composition, thereby affecting the local chemistry. Chemical reactions, in turn, affect the flow field primarily by way of change in local density due to heat release. Because of the high temperature of combustion systems radiative heat transfer also becomes important. All these three subproblems intimately interact with each other in combustion systems. Each of these subphysics are computationally very intensive and complex. When the problem of soot formation and growth is added to the mix, the complexity of the system is further increased.

Our knowledge of the exact physical processes involved in soot evolution is limited. In recent years rigorous experimental and computational research related to soot formation and growth in combustion systems has provided important insights into the physics of the problem [4, 5, 12, 14, 31, 36]. The formation of soot is always preceded by formation of polycyclic aromatic hydrocarbons (PAH). It is accepted that PAHs are the incipient species for soot. Once formed, soot particles undergo several physical and chemical processes. Local gas-phase species not only acts as the nucleating species, but also condenses on the surface of existing 0soot particles, thereby increasing the soot particle size. This process is called P AH condensation. The second physical process is called coagulation, which refers to

the Brownian collision of soot particles. The most strong chemical process is that of surface reaction of soot with gas-phase species such as H, O_2, C_2H_2, and OH. It is commonly accepted that interaction with H creates radical sites on the soot surface with which C_2H_2 reacts and contributes to growth of soot'. These surface radical sites are also the sites with which gas-phase oxidizer species react leading to decrease in soot mass. This chemical process is called soot surface reaction.

Based on the current understanding, several empirical, semi-empirical, and detailed models for soot has been developed by various researchers. Empirical soot models model soot formation in a combustion system from a purely phenomenological point of view and are computationally least expensive. Semi-empirical models account for a very simplistic physics of soot formation and growth in the combustion system and are widely used in device-scale simulations because of their low computational cost. Detailed soot models, on the other hand, try to capture the physics and chemistry of soot evolution to the extent they are known. Because of the high computation cost, use of detailed soot models are limited in device-scale simulations. A comprehensive review of soot models can be found in [16].

Despite recent advances, fully-coupled simulations of flow, chemistry, radiation, and soot evolution in combustion systems are still rare. The main limitations of such studies are twofold. First, models of soot formation and growth suffers from our lack of understanding of fundamental physics of soot evolution. The uncertainty associated with soot models often becomes bottleneck in interpreting the complex interactions between soot, chemistry, flow field, and radiation [25, 33]. Second, a high-fidelity simulation with detailed accurate models for each of the subphysics (i.e., fluid dynamics, chemistry, radiation, and soot evolution) is numerically cost prohibitive. Each of these subphysics are computationally very costly, and a fully coupled simulation, often is limited to laboratory scale small flames [26, 27].

The current work aims to partially address both of the above issues. First, a semi-empirical soot model and a detailed soot model are implemented on a laminar flame solver. This is used to study an axisymmetric laminar diffusion sooting flame, for which extensive experimental data are available. This study is expected to validate the soot model as well as provide valuable insights in the soot evolution in laminar flames. Second, a detailed soot model is implemented on a fully coupled turbulent flame solver for Reynolds-averaged simulation (RAS) to study effect of interaction of turbulence with soot, chemistry, and radiation. Because of the high computation cost, high-fidelity modeling of soot, in either laminar or turbulent flames, require access to reliable and state-of-the-art computational resources. The current study was primarily done on the SDSC Trestles cluster.

The work presented here is still under progress. In this article only the preliminary results from the laminar flame solver and a scaling study of the turbulent flame solver is reported. In the next section we briefly discuss the numerical models used in the current study followed by a discussion on the target configurations. Then the preliminary results are presented. Finally a occlusion is drawn and some future study directions are presented.

2. NUMERICAL MODEL

In this work two soot models are considered - a semiempirical model [10, 21] and a detailed model using method of moments with interpolative closure (MOMIC) [8]. The semi-empirical two-equation soot model chosen is based on an earlier model by Leung et al. [21]. In this model, two transport equations are solved for soot number density (N_s) and the soot mass fraction (Y_s). In current study, the model of Leung et al. is used with the additional effects of soot oxidation by OH and O based on the work of Guo et al. [10]. The transport equations for soot scalars in the semiempirical model is given as:

$$\frac{\partial_\rho Y_s}{\partial t} + \frac{\partial}{\partial x_j}\left(\rho u_j Y_s\right) = \frac{\partial}{\partial x_j}\left(\frac{\mu}{Sc}\frac{\partial Y_s}{\partial x_j}\right) - \frac{\partial}{\partial x_j}\left(\rho V_{T,j} Y_s\right) + S_m,$$

(1)

$$\frac{\partial_\rho N_s}{\partial t} + \frac{\partial}{\partial x_j}\left(\rho u_j N_s\right) = \frac{\partial}{\partial x_j}\left(\frac{\mu}{Sc}\frac{\partial N_s}{\partial x_j}\right) - \frac{\partial}{\partial x_j}\left(\rho V_{T,j} N_s\right) + S_N,$$

(2)

where $\mathbf{V}_T$ is the thermophoretic diffusion velocity for soot, and is defined as $V_{T,i} = -0.54\,\frac{\mu}{\rho T}\frac{\partial T}{\partial x_i}$, $\mathbf{u}$ is the gas-phase velocity, ρ is the gas-phase density, μ is the viscosity, and S_m and S_N are the source terms that account for the formation, growth and oxidation of soot particles. The original formulation [10, 21] does not have the molecular diffusion term for the equations; these have been added for numerical stability with the assumption of large effective Schmidt number $(Sc >> 1)$ for soot [32].

The detailed soot model considered in this work is the well-established method of moments with interpolative closure (MOMIC) proposed by Frenklach and coworkers [8]. In MOMIC the concentration moments of the soot particle size distribution function (PSDF) are solved explicitly taking into account nucleation, condensation, coagulation, and surface growth. The concentration moments of PSDF are defined as

$$M_r = \sum_{i=l}^{\infty} m_i^r N_i,$$

where m_i is the number of carbon atoms in the soot particles of size class i, and N_i is the number density of that size class. Mathematically the unique PSDF can be reconstructed by solving for complete set of moments. In practice, for numerical tractability, only first few low-order moments are solved using an appropriate closure scheme. In this work, first six concentration moments $(M_0 - M_5)$ are used. The PAH participating in MOMIC was considered to be pyrene (A$_4$, $C_{15}H_{10}$) for the current study. The soot surface reactions were based on the H-abstraction-C$_2$H$_2$-addition (HACA) reaction pathway proposed by Frenklach and coworkers [2, 8]. The complete description of the MOMIC can be found in [8, 32].

The flame solvers used in this study is developed based on the open-source CFD toolbox **OpenFOAM** [I]. The main flow solver is a pressure-based solver. Both the laminar and turbulent flame solvers are built around this main flow solver.

The laminar flame solver solves the coupled momentum, sensible enthalpy and species mass fraction equations along with the soot scalars *(N_s and Y_s for semi-empirical model and moments for MOMIC).* The model uses a segregated time-marching algorithm. The effects of differential diffusion are explicitly considered in species and enthalpy transport equation. A mixture-averaged model is used to compute the transport properties for the gas-phase species and mass conservation is ensured by using a correction-velocity formulation [15, 20]. The chemical kinetics source terms are calculated using the stiff ODE solver CVODE [7, 13]. An optically thin radiation model [3, 10] is used for the energy equation. The model is an emission-only model, and radiation from CO_2, H_2O, CO, CH_4 and soot is included in the model.

The turbulent flame solver is for Reynold-averaged simulations (RAS) of turbulent reacting flows. Due to closure problems associated with Reynolds-averaged turbulent transport equations, the turbulent flame solver requires special treatment for species and energy transport. In this study we used a transported probability density function (tPDF) method for this purpose. The tPDF method provides convenient and accurate closure for chemical and enthalpy source terms using a Lagrangian stochastic scheme. The Lagrangian scheme of tPDF method is implemented on the Eulerian finite volume grid used by the **OpenFOAM** flow solver in consistently coupled fashion. The **OpenFOAM** flow solver solves for the flow field and the tPDF module solves for the species and energy transport. The flow solver and the tPDF module exchanges information at each time step and performs rigorous consistency checks at step. The complete description of the tPDF-based RAS solver can be found in [11]. The radiation source terms for the energy equation is obtained by solving the radiative transfer equation (RTE) using a high-fidelity photon Mote-Carlo (PMC) method with line-by-line spectral database for CO_2, H_2O, CO, and soot. The details of the radiation model can be found in [28, 30]. Parts of the tPDF and PMC modules were previously validated in various other code suites [26, 27, 39].

Both the solvers use a first order scheme to march the solution in time starting from an initial condition. In the laminar flame solver an apparent Schmdit number of 60 was used for diffusion of soot particles. In the turbulent flame solver diffusion of soot moments was modeled using the size independent formulation as reported in [32].

The solution of species transport equations in both the laminar and turbulent flame solver require to solution of systems of stiff ordinary differential equations (ODEs) to obtain the chemical source terms. Solution of stiff ODEs are computationally the most costly step in the solution algorithm. However, these ODEs are local in nature and hence demands little communication overhead. Additionally the turbulent flame solver calls for non-local particle tracking and photon Monte-Carlo schemes.

The laminar flame solver was developed on **OpenFOAM** - 1.7, whereas the turbulent flame solver was developed on **OpenFOAM** -2.2.x. Both the solver uses the message passing interface (MPI) as the parallel communication protocol.

3. TEST CONFIGURATIONS

One laminar axisymmetric diffusion flame and one turbulent jet flame of ethylene and air was chosen for the current study. The target laminar flame is the atmospheric-pressure ethylene flame studied experimentally by Santoro et al. [34]. The burner consists of a 11.1 mm diameter inner fuel tube and an outer 102 mm diameter tube for the air co-flow. Honeycomb structures and glass beads are used to obtain a uniform flow velocity of fuel and air. The fuel nozzle extends upto a distance of 4 mm into the air flow. Out of several flames studied by Santoro et al. [34], we considered the one with the fuel flow rate of 3.85 cc/sec and the air flow rate of 713.3 cc/sec. These conditions correspond to the non-smoking case of Santoro et al., wherein the soot is completely oxidized within the flame. An uncertainty of approximately ±20% is given for the experimental data for the gas-phase species while for OH, the uncertainty is about 50% [17].

The turbulent sooting flame chosen for the current study was studied by Lee et al. [19]. The flame consists of ethylene jet from a central fuel tube of 2.18 mm inner diameter surrounded by a concentric outer tube of 15. 75 mm diameter, which provides a pilot of hydrogen for flame anchoring. The Reynolds number at the cold jet exit is 12,000. Detailed measurements of both mean quantities and PDFs of soot volume fraction, OH, and PAH for this flame can be found in [19].

A total of six gas-phase chemical mechanisms for ethylene (listed in Table 1) were used in this study. Since the

Table 1: List of gas -phase mechanisms used.

Mechanism	Species	Reactions	PAH	Reference
LYR32	32	206	No	[22]
QLY33	33	205	No	[18]
QLY70	70	463	No	[29]
WL75	75	529	No	[38]
WF99	99	533	Yes	[9]

semi-empirical soot model does not account effect of PAHs on soot evolution, only first five mechanisms were used with this soot model. By the same logic, only WF99 mechanisms was used with the detailed MOMIC soot model which treats PAH as the precursor of soot. Since computational effort scales directly with size of the gas-phase mechanism, for preliminary tests in the turbulent flame only the small QLY33 mechanism was used. The choice of this mechanism for turbulent flame simulation is based on detailed assessment of mechanisms as reported in [25].

The simulations were performed using axisymmetric wedge shaped meshes. Non-uniform meshes were used, so that higher grid resolution can be achieved in areas where mixing and reactions take place. The domain of the laminar flame was discretized with 12400 cells, with smallest grid size being around 0.1 mm. The domain of the turbulent flame domain was discretized with 5940 cells with smallest grid size being 0.2mm.

The laminar flame simulations were done on Trestles clusters using 48 processors for the two-equation soot model, and 128 processors for the MOMIC soot model. The scaling study of the turbulent flame solver was done on a local cluster. The validation of the turbulent solver is being done on both local clusters and the Trestles cluster.

4. RESULTS AND DISCUSSION

In this section we first discuss preliminary results from the laminar flame simulation using both the semi-empirical two-equation soot model as well as the MOMIC. We use key gas-phase species concentration and soot volume fraction measurements as our first-order assessment of model validation. In the end we present results from scaling study for both the laminar and turbulent flame solver.

The overall the agreement with experimental data is quite good. Figures 1 and 2 show the results obtained from the two-equation soot model using the first five gas-phase mechanisms listed in Table 1. We only report radial profiles of various scalars at one location. Profiles at other locations show similar trends.

While all mechanisms predict very similar radial evolution of OH, the prediction of C_2H_2 is quite varied. Since C_2H_2 is the key inception species in the semi-empirical soot model, this variation on C_2H_2 prediction results in variation in predicted soot volume fraction across the gas-phase-mechanisms. However, for most part, the computed results are within the experimental uncertainty.
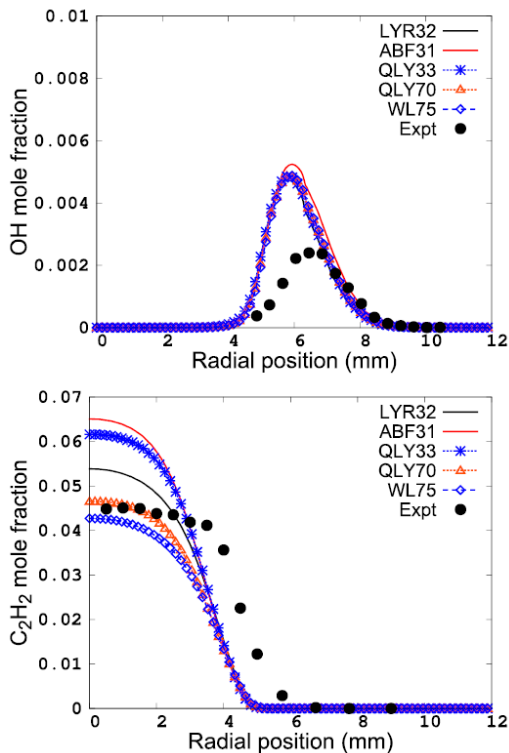

Figure 1: OH and C2H2 profiles 20 mm from nozzle using the two-equation soot model.

The soot volume fraction profiles are very well predicted, especially in view of the simple chemistry, soot and radiation models in use. Accurate predictions of the gas-phase species is dependent on the chemical kinetics model used, and this in turn affects the soot predictions. In addition, the radiation modeling also has a big effect on the soot production as reported by other researchers [26, 27]. Consistent to reported findings, the optically thin radiation model used in the current work demonstrate a strong effect on flame – at the locations where the model overpredicts the soot volume fraction, the temperature is underpredicted. This points to the requirement of implementation of a more accurate radiation model in this solver. This, however, is left as a future work for now.

Figure 3 shows the computed soot volume fractions by the detailed MOMIC model. As in the two-equation model results, the results from the initial simulations with the MOMIC soot model are promising. The peak soot volume fractions at the axial locations are captured by the model. With this model, we have also performed a sensitivity study on soot volume fraction with PAH condensation. Clearly, consideration of PAH condensation affects the soot volume fraction. Since condensation consumes the PAH, which is the inception species for soot nucleation, inclusion of condensation reduces the overall soot production. This is consistent with observations reported in [33, 37].

Finally, the scalability of the solvers were investigated. A strong-scaling study was performed using the 32-species chemical mechanism on 8, 16, 32, and 64 cores. Due to the computational cost of the simulations, these tests were not run to a full steady state; rather each case was run for a
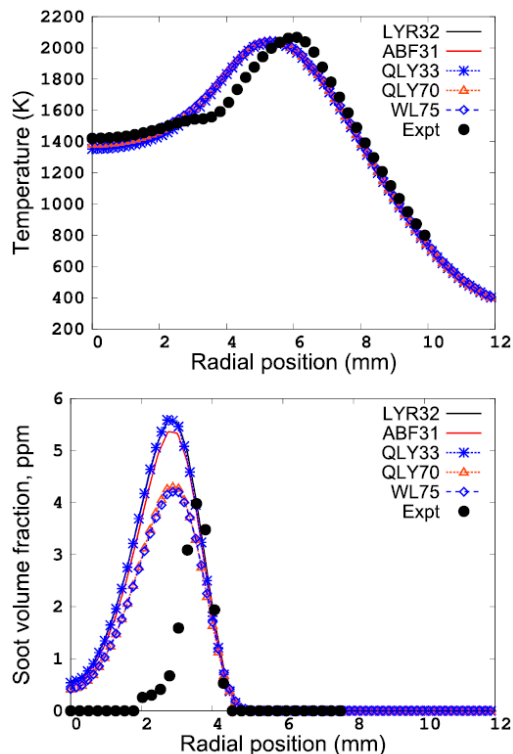

Figure 2: Temperature and soot profiles 20 mm from nozzle using the two-equation soot model.
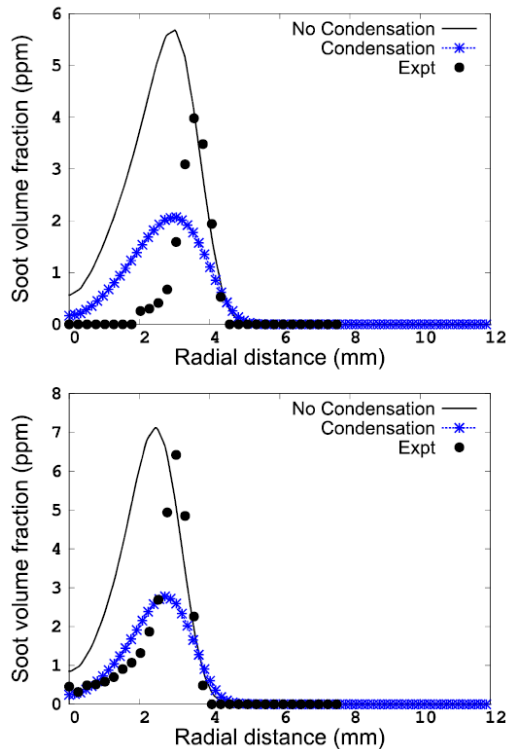
Figure 3: Soot profiles for the MOMIC soot model at various heights from the nozzle.
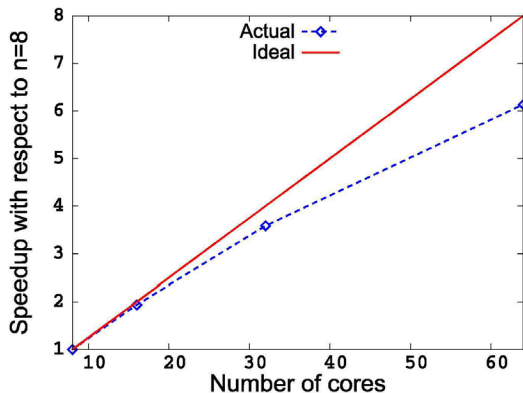

Figure 4: Strong scaling results for a relatively small axisymmetric laminar flame problem

specified amount of physical time, and the corresponding wall time was noted. Of interest in these tests is the ratio of the wall time using 8 processors to the wall time using n processors. For this problem, the speedup using 64 processors is seen to be about 6.2, and the parallel efficiency is more than 80% for $n \leq 64$. Because the computational cost increases with the size of the chemical mechanism used for larger mechanisms (~ 100 species) the speedup (relative to 8 processors) is expected to be even more.

The turbulent flame solver, as discussed before, is built using previously validated modules. The experimental validation of the turbulent solver with the target flame [19] is still a work in progress. Here we only show a result from a strong scaling study of the solver similar to the one done with the

laminar flame solver. In this case the base case was taken as the case on $n = 2$ processors and speedup using 8, 16, 32, 64, and 96 processors were estimated in the way similar to the one described previously. This scaling was done on a grid size of 5940 cells using the QLY33 mechanism with MOMIC. The scaling study was done without any radiation model to capture the efficiency of chemistry scaling. A study on efficiency of scaling of radiation model is under progress.
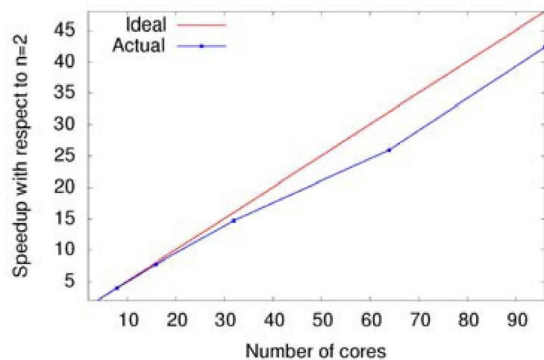

Figure 5: Strong scaling results for a relatively small axisymmetric turbulent jet flame with soot model.

As can be seen from Fig. 5, the RAS-tPDF implementation scales very well up to 96 processors for the chosen problem size. The parallel efficiency of approximately 80% is observed at 96 processors. The high scalability of the solver is primarily due to the fact that ODEs for chemical source term is local to every cell. With radiation model, the scaling efficiency is expected to reduce, but not drastically. The PMC model has been previously shown to be computationally very efficient [28, 30]. But involvement of nonlocal component in the radiation source term as well as tracking of photon rays is expected to affect negatively on the scaling efficiency. However, it has been found previously in a similar turbulent flame solver that the total time taken for solving the radiative transfer equation is much less compared to that for solving the chemistry, i.e., the species transport equation [24]. Therefore, we do not expect that inclusion of radiation will affect the scalability drastically.

5. CONCLUSION AND FUTURE STUDIES

The current work attempts to develop and validated a laminar flame solver and a turbulent flame solver with detailed soot models and radiation models. As part of this work, first, a model for simulating axi-symmetric laminar diffusion flames was developed. A mixture-averaged model was used to compute the transport properties of the gas-phase species, and the effects of differential diffusion of mass and energy were taken into account. A semi-empirical two-equation soot model and a detailed MO MIC soot model were implemented in the solver and were subsequently validated against experimental data for a laboratory-scale ethylene diffusion flame. Both the soot models were able to capture the essential features of the sooting characteristics of the flame. Effect of PAH condensation on the soot volume fraction was also studied on the laminar flame using the MOMIC. An optically thin radiation model was also used in this work. As the next step, a turbulent flame solver is being developed using previously validated modules for detailed soot model and radiation model. The validation of the turbulent solver is under progress.

Strong-scaling studies of both the laminar and turbulent flame solvers were performed. The laminar flame solver showed good speedup up to 64 processors, whereas the turbulent solver showed good speedup up to 96 processors for the species transport calculations. Use of larger chemical mechanisms is expected to scale well up to an even larger number of processors.

Since accurate prediction of soot require large gas-phase chemical mechanisms and detailed soot model with detailed radiation model, requirement of highly scalable laminar and turbulent flame solver can never be overstated. After complete validation of the solvers discussed in this work we intend to perform an exhaustive and systematic study of target flames mentioned in this work as well as other target flames. Eventually, we wish to simulate high-pressure laboratory-scale laminar and turbulent flames as most of the practical combustion systems of interest work under elevated pressure.

6. ACKNOWLEDGEMENT

References

[1] **OpenFOAM**. www.OpenFOAM.com, 2010.

[2] J. Appel, H. Bockhorn, and M. Frenklach. Kinetic modeling of soot formation with detailed chemistry and physics: Laminar premixed flames of C2 hydrocarbons. *Combust. Flame,* 121:122 - 136, 2000.

[3] R. S. Barlow, A. N. Karpetis, J. H. Frank, and J. Y. Chen. Scalar profiles and NO formation in laminar opposed-flow partially premixed methane/air flames. *Combustion and Flame,* 127:2102- 2118, 2001.

[4] H. Bockhorn. *Soot Formation in Combustion: Mechanisms and Models.* Springer-Verlag, New York, 1994.

[5] H. Bockhorn, A. D'Anna, A. F. Sarofim, and H. Wang. *Combustion Generated Fine Carbonaceous Particles.* KIT Scientific Publishing, Karlsruhe, 2009.

[6] T. C. Bond, S. J. Doherty, D. W. Fahey, P. M. Forster, T. Berntsen, B. J. DeAngelo, M. G. Flanner, S. Ghan, B. Karcher, D. Koch, S. Kinne, Y. Kondo, P. K. Quinn, M. C. Sarofim, M. Schultz, M. G. Schulz, C. Venkataraman, H. Zhang, S. Zhang, N. Bellouin, S. K. Guttikunda, P. K. Hopke, M. Z. Jacobson, J. W. Kaiser, J. Klimont, U. Lohmann, J. P. Schwarz, D. Shindell, T. Storelvmo, S. G. Warren, and C. S. Zender. Bounding the role of black carbon in the climate system: A scientific assessment. *J. Geophys. Res. Atmos.,* 118:1 - 173, 2013.

[7] D. C. Cohen and A. C. Hindmarsh. Cvode, a stiff/ nonstiff ode solver inc. In *SciCADE95: scientific computing and differential equations,* 1995.

[8] M. Frenklach. Method of moments with interpolative closure. *Chemical Engineering Science,* 57:2229-2239, 2002.

[9] M. Frenklach and H. Wang. A detailed kinetic modeling study of aromatics formation in laminar premixed acetylene and ethylene flames. *Combustion and Flame,* 110:173‑ 221, 1997.

[10] H. Guo, F. Liu, and G. J. Smallwood. Soot and no formation in counterflow ethylene/oxygen/ nitrogen diffusion flames. *Combustion Theory and Modeling,* 8:475-489, 2004.

[11] D. C. Haworth. Progress in probability density function methods for turbulent reacting flows. *Prag. Energy Combust. Sci.,* 36:168‑ 259, 2010.

[12] B. S. Haynes and H. G. Wagner. Soot formation. *Prag. Energy Combust. Sci.,* 7:229‑ 273, 1981.

[13] A. C. Hindmarsh and R. Serban. User documentation for cvode v 2.7.0. Technical report, Lawrence Livermore National Laboratory, 2012.

[14] A. E. Karataş and Ö. L. Gtilder. Soot formation in high pressure laminar diffusion flames. *Prag. Energy Combust. Sci.,* 38:818‑ 845, 2012.

[15] R. J. Kee, G. Dixon-Lewis, J. Warnatz, M. E. Coltrin, and J. A. Miller. A fortran computer code package for the evaluation of gas phase multicomponent transport properties. Sand86-8246 unlimited release, Sandia National Laboratory, 1986.

[16] I. M. Kennedy. Models of soot formation and oxidation. *Prag. Energy Combust. Sci.,* 23:95‑ 132, 1997.

[17] I. M. Kennedy, C. Yam, D. C. Rapp, and R. J. Santoro. Modeling and measurements of soot and species in a laminar diffusion flame. *Combustion and Flame,* 107:368‑ 382, 1996.

[18] C. K. Law. Comprehensive description of chemistry in combustion modeling. *Combustion Science and Technology,* 177:845‑ 870, 2005.

[19] S. Y. Lee, S. R. Turns, and R. J. Santoro. Measurements of soot, OH, and PAH concentrations in turbulent ethylene/air jet flames. *Combust. Flame,* 156:2264‑ 2275, 2009.

[20] S. Lei, J. Cai, M. F. Modest, A. Dasgupta, and D. C. Haworth. Photon Monte Carlo model for high-pressure reacting laminar flows. In *Proceedings of the ASME 2012 International Mechanical Engineering Congress & Exposition,* 2012.

[21] K. M. Leung, R. P. Lindstedt, and W. P. Jones. A simplified reaction mechanism for soot formation in non premixed flames. *Combustion and Flame,* 87:289-305, 1991.

[22] Z. Luo, C. S. Yoo, E. S. Richardson, J. H. Chen, C. K. Law, and T. F. Lu. Chemical explosive mode analysis for a turbulent lifted ethylene jet flame in highly-heated coflow. *Combustion and Flame,* 159:265‑ 274, 2011.

[23] MECHMOD. http://garfield.chem.elte.hu/Combustion/mechmod.htm, 2010.

[24] R. S. Mehta. *Detailed Modeling of Soot Formation and Turbulence - Radiation Interactions in Turbulent Jet Flames.* Ph.cl. diss., The Pennsylvania State University, University Park, PA, USA, 2008.

[25] R. S. Mehta, D. C. Haworth, and M. F. Modest. An assessment of gas-phase reaction mechanisms and soot models for laminar atmospheric-pressure ethylene-air flames. *Proc. Combust. Inst.,* 32:1327‑ 1337, 2009.

[26] R. S. Mehta, D. C. Haworth, and M. F. Modest. Composition PDF / photon Monte Carlo modeling of moderately sooting turbulent jet flames. *Combust. Flame,* 157:982‑ 994, 2010.

[27] R. S. Mehta, M. F. Modest, and D. C. Haworth. Radiation characteristics and turbulence-radiation interaction in sooting turbulent jet flames. *Combust. Theory Modell.,* 14:105‑ 124, 2010.

[28] G. Pal. *Spectral Modeling of Radiation in Combustion Systems.* Ph.cl. diss., The Pennsylvania State University, University Park, PA, USA, 2010.

[29] Z. Qin, V. V. Lissianski, H. Yang, W. C. Gardiner, S. G. Davis, and H. Wang. Combustion chemistry of propane: A case study of detailed reaction mechanism optimization. In *Proceedings of the Combustion Institute,* volume 28, pages 1663- 1669, 2000.

[30] T. Ren and M. Modest. A hybrid wavenumber selection scheme for line-by-line photon Monte Carlo simulations in high-temperature gases. *J. Heat Transfer,* 135:084501(1) - 084501(4), 2013.

[31] H. Richter and J. Howard. Formation of polycyclic aromatic hydrocarbons and their growth to soot - a review of chemical reaction pathways. *Prog. Energy Combust. Sci.,* 26:565 - 608, 2000.

[32] S. P. Roy, P. G. Arias, V. Lecoustre, H. G. Im, D. C. Haworth, and A. Trouve. Development of high fidelity soot aerosol dynamics models using method of moments with interpolative closure. *Aerosol Sci. Technol.,* 48:379 - 391, 2014.

[33] S. P. Roy and D. C. Haworth. Comparisons of section and moment-based soot aerosol dynamics models for laminar premixed ethylene flames. *Combust. Theory Model.* Under review.

[34] R. J. Santoro, H. G. Semerjian, and R. A. Dobbins. Soot particle measurements in diffusion flames. *Combustion and Flame,* 51:203- 218, 1983.

[35] U.S. EPA. Integrated science assessment for particulate matter (final report). Technical Report EPA/600/R-08/139F, U.S. Environment Protection Agency, Washington, DC, 2009.

[36] H. Wang. Formation of nascent soot and other condensed-phase materials in flames. *Proc. Comb. Inst.,* 33:41 - 67, 2011.

[37] H. Wang, D. X. Du, C. J. Sung, and C. K. Law. Experiments and numerical simulation on soot formation in opposed-jet ethylene diffusion flames. In *Twenty-Sixth Symposium on Combustion/The Combustion Institute,* pages 2359- 2368, 1996.

[38] H. Wang and A. Laskin. A comprehensive kinetic model of ethylene and acetylene oxidation at high temperatures. Technical report, AFOSR, 1991.

[39] X. Y. Zhao, D. C. Haworth, and E. D. Huckaby. Transported pdf modeling of non-premixed turbulent co/H2/N2 jet flames. *Combustion Science and Technology,* 184:676-693, 2012.